ACS OMEGA

http://pubs.acs.org/journal/acsodf

Article

Investigation of Nanoclay-Surfactant-Stabilized Foam for Improving Oil Recovery of Steam Flooding in Offshore Heavy Oil Reservoirs

Wei Zheng,* Xianhong Tan, Weidong Jiang, Haojun Xie, and Haihua Pei

Cite This: *ACS Omega* 2021, 6, 22709−22716

Read Online

ACCESS | Metrics & More | Article Recommendations

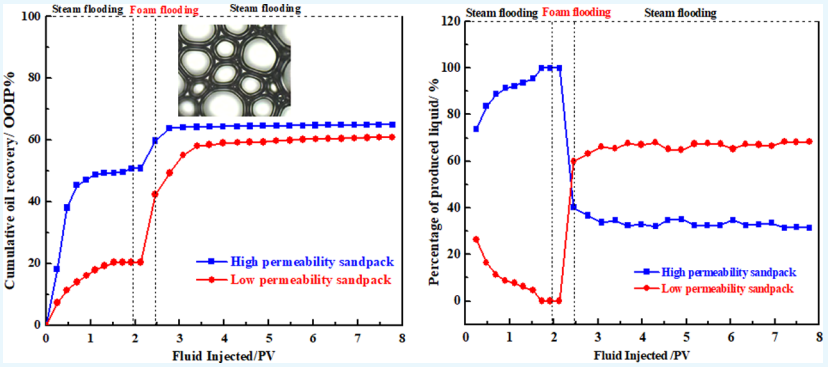

ABSTRACT: This study presents a study of nanoclay-surfactant-stabilized foam to improve the oil recovery of steam flooding in offshore heavy oil reservoirs. The foam stability and thermal resistance studies were first performed to investigate the influence of nanoclay on the stability and thermal resistance properties of the foam system. Then, the sandpack flooding tests were conducted for investigating the resistance factor and displacement abilities by nanoclay-surfactant-stabilized foam. The results showed that the nanoclay-surfactant-stabilized foam has excellent foaming ability and foam stability at 300 °C, which can be used in steam flooding for offshore heavy oil reservoirs. The resistance factor is greater than 30 at 300 °C when the gas−liquid ratio ranges from 1 to 3, which indicated that the nanoclay-surfactant-stabilized foam has good performance of thermal resistance and plugging effect. The heterogeneous sandpack flooding test showed that the nanoclay-surfactant-stabilized foam can effectively divert the steam into the low-permeability area and improve the sweep efficiency, thus improving heavy oil recovery of steam flooding. Therefore, the nanoclay-surfactant-stabilized foam flooding has a great potential for improving oil recovery of steam flooding in offshore heavy oil reservoirs.

1. INTRODUCTION

China has abundant heavy oil reserves in offshore oilfields, and the steam-injection thermal method is currently one of the effective technologies to exploit in offshore heavy oil. Since 2008, the pilot experiment of multielement thermal fluid and steam stimulation has been carried out and achieved good development results. In order to promote the development of large-scale thermal recovery of offshore heavy oil, China's first offshore thermal recovery platform was successfully put into operation in September 2020, marking that China's offshore thermal recovery has entered the stage of large-scale thermal recovery from the pilot test stage. However, due to the low steam density and viscosity, it is easy to cause steam overriding, steam channeling, and fingering phenomenon in the heterogeneous formations, which reduces the sweep efficiency of steam flooding and thus lowers the oil recovery of steam flooding.

Foam-assisted steam flooding is an effective technology to improve the sweep efficiency of steam flooding by inhibiting the steam channeling and gravity override, thus increasing the oil recovery of steam flooding.[1−3] The high-temperature foam agent can not only inhibit the steam overriding but also reduce the steam mobility. Besides, the foam also has the selective blocking characteristics, which can block the big pores rather than the small pores and block the water layers rather than the oil layers.[4,5] It is indicated that the foam is an ideal high-temperature profile control and flooding agent, and thus, foam is widely used in steam flooding for improving heavy oil recovery.[6,7] The experimental results by Bagheri and Clark showed that foam-assisted steam flooding could achieve good results, which verified the application prospect of foam-assisted

Received: June 8, 2021
Accepted: August 10, 2021
Published: August 24, 2021

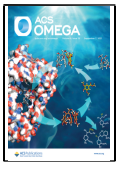

https://doi.org/10.1021/acsomega.1c03008
ACS Omega 2021, 6, 22709−22716

Table 1. Composition of Formation Water in Offshore Oilfield

ion concentration/(mg/L)								
Na^+	K^+	Mg^{2+}	Ca^{2+}	Cl^-	SO_4^{2-}	HCO_3^-	CO_3^{2-}	total salinity/(mg/L)
2004	506	77	279	3211	466	670	20	7233

(a) Warring Blender (b) Foam volume (c) Liquid drainage half-life time (d) Foam half-life time

Figure 1. Schematic diagram of measurements of foaming ability and foam stability. (a) Warring Blender, (b) foam volume, (c) liquid drainage half-life time, (d) foam half-life time.

steam flooding in the Canadian thermal recovery project being developed in northwest Alberta.[8] Wang et al. carried out physical simulation experiments to prove that the flue gas foam-assisted steam flooding technology had a good ability to improve the recovery of steam flooding.[9,10]

It is well-known that the foam thermal stability is the key problem in steam flooding to improve the sweep efficiency. In general, the polymer has been widely used for foam stabilizers to improve the foam stability. However, the polymer molecule can be usually be degraded under high temperature conditions, thus losing the ability to stabilize foam.[11−13] As a result, the research on foam stabilization technology is gradually moving toward the development of inorganic nanoparticle as foam stabilizers.[14−19] Yekeen found that the stability of SDS foam could be effectively improved with the addition of silica nanoparticles.[20] Khajehpour showed that the silica nanoparticles can not only increase the stability of the foam but also increase the thermal resistance of the foam.[21] Some other researchers improved CO_2 foam performance by adding the silica nanoparticles as a foam stabilizer.[22−26] Rezaei put forward and demonstrated a N_2 foam combination of CAPB (0.05 wt %) + SiO_2 (0.1 wt %) + NaCl (5.0 wt %) that could form more stable foams.[27]

Due to the high speed and high efficiency in offshore oilfield development requirement, large well spacing and large-section joint production are generally adopted, so it is more important to maintain balanced displacement requirements. A high-temperature foam system is an effective technology to inhibit the steam channeling and gravity override to improve the oil recovery of steam flooding. However, the ordinary polymer-stabilized foam system cannot be stable at a high temperature of 300 °C. Although nanoparticle-stabilized foam has excellent foam stability and mobility control ability at a high temperature of 300 °C, the nanoparticle surface needs to be modified to adsorb at the gas−liquid interface. Besides, the surface modification of nanoparticles is relatively complicated and the modified nanoparticles are easy to agglomerate in water. In view of the abovementioned problems and the shortcomings of the existing technology, the nanoclay-surfactant-stabilized foam system was proposed for improving the recovery of steam flooding in offshore oilfields. In this study, the nanoclay-surfactant-stabilized foam system which can be used at 300 °C was prepared by a sulfonate surfactant α-AOS and nanoclay particle NMT and the foam performance, thermal resistance, plugging performance, and enhanced oil recovery of the system were evaluated in this study.

2. EXPERIMENTS AND METHODS

2.1. Experimental Materials. The heavy oil and formation brine were collected from heavy oil reservoirs in offshore oilfield, China. The viscosity of the oil is 1578 mPa·s and the density is 0.981 g/cm^3 at 40 °C. The analysis of the formation brine is shown in Table 1. All the solutions used in the experiments were prepared with synthesized formation brine according to Table 1. The chemical agents used in this study included surfactant and nanoclay particles. A sulfonate surfactant sodium α-olefin (α-AOS, provided by Shandong Usolf Chemical Technology) was used as a foaming agent, and a nanoclay particle (NMT) with an average diameter of 30−50 nm was used as a foam stabilizer.

2.2. Measurements of Foaming Ability and Foam Stability. In this study, the Warring Blender method was used to evaluate the foaming ability and foam stability. The foaming ability and foam stability of the surfactant were evaluated by measurements of foaming volume, liquid drainage half-life time, and foam half-life time. A total of 100 mL of foaming system solution was injected into a blender as shown in Figure 1a and agitated for 60 s at a speed of 3000 rpm. The maximum foam volume was measured, and the foam drainage began. When the liquid drainage volume reached 50 mL, the half time of the liquid drainage was recorded. When the foam volume reached the half of the maximum foam volume, the foam half time was recorded. These recording points are as shown in Figure 1.

2.3. Measurements of the Foam Resistance Factor. A series of sandpack flooding tests were conducted with a permeability of 2000 mD to determine the foam resistance factor at a temperature of 300 °C. The experimental procedures were as follows: At first, the steam and nitrogen were coinjected at different gas−liquid ratios and the pressure drop ΔP_1 was recorded. Then, steam, foam system solution, and nitrogen were coinjected with different gas−liquid ratios and the pressure ΔP_2

https://doi.org/10.1021/acsomega.1c03008
ACS Omega 2021, 6, 22709−22716

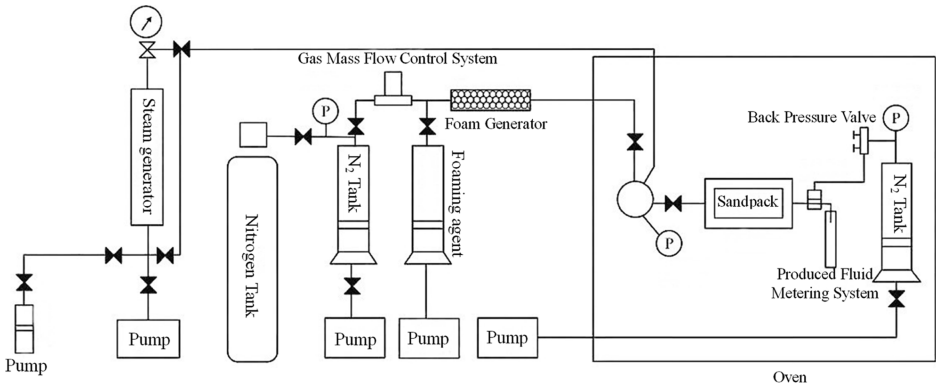

Figure 2. Schematic of sandpack flooding test for foam-assisted steam flooding.

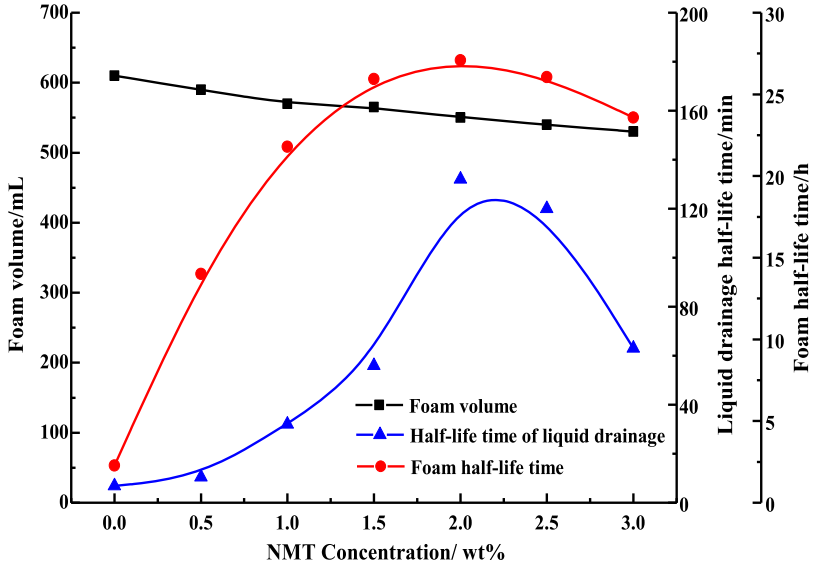

Figure 3. Foam ability and foam stability of AOS with different concentrations.

was recorded. The resistance factor was calculated using formula $R = \Delta P_2/\Delta P_1$.

2.4. Sandpack Flooding Tests. A single sandpack flooding and the parallel double sandpack flooding tests with different permeabilities were carried out to evaluate the effectiveness of nanoclay-stabilized foam for improved oil recovery of steam flooding. The sandpack used in this study was 30 cm in length and 2.5 cm in diameter. The sandpack with a permeability of 878−2533 mD was packed by quartz sands with a size of 80−100 and 100−200 meshes. The experimental procedure was briefly described as follows: the sandpack was first saturated with the synthesized formation brine and then saturated with the heavy oil at 40 °C. After the sandpack was aged for 24 h, the steam flooding at 300 °C was performed until the water cut was greater than 98%, and then, a 0.5 PV slug of nanoclay-stabilized foam was injected at a gas−liquid ratio of 1:1. Subsequent steam flooding at 300 °C was conducted until the oil production ceased. Schematic of the sandpack flooding test for foam-assisted steam flooding is shown in Figure 2.

3. RESULTS AND DISCUSSION

3.1. Foaming Ability and Foam Stability. *3.1.1. Evaluation of the Surfactant-Foaming Agent.* Figure 3 shows the foam ability and foam stability of surfactant AOS with different concentrations. It can be seen that the foaming ability gradually increased with the increase in the concentration of AOS and the half-life time of the liquid drainage and the foam half-life time first increased and then decreased with increasing concentration. When the concentration of AOS was low, the surface tension between gas−liquid phases was high, and part of the foam generated was broken in a transient time, so the foam volume was manifested as small. As the concentration of AOS increased, the surface tension of the gas−liquid phase decreased gradually, the volume of instantaneously broken foam decreased, so the foam volume increased significantly. The stability of foam depends on the stability of the foam liquid film, and it is also affected by liquid viscosity, Marangoni effect, surface charge of the liquid film, and other factors. The stability of the foam liquid film is mainly affected by the electrostatic force between surfactant molecules, van der Waals force, hydrogen bond, steric resistance, and viscoelasticity of the surface film.[28−30] For AOS surfactants, as the concentration increases, the density and arrangement of the AOS on the liquid film will change, which will extend the half-life time of liquid drainage and the foam half-life time through electrostatic force and van der Waals force.

3.1.2. Evaluation of Nanoclay-Surfactant-Stabilized Foam. In order to study the effect of added nanoclay on the stability of the surfactant-stabilized foam system, a series of foaming agents were prepared with 0.5 wt % AOS with different concentrations of nanoclay (NMT). Figure 4 shows the foaming ability and

https://doi.org/10.1021/acsomega.1c03008
ACS Omega 2021, 6, 22709−22716

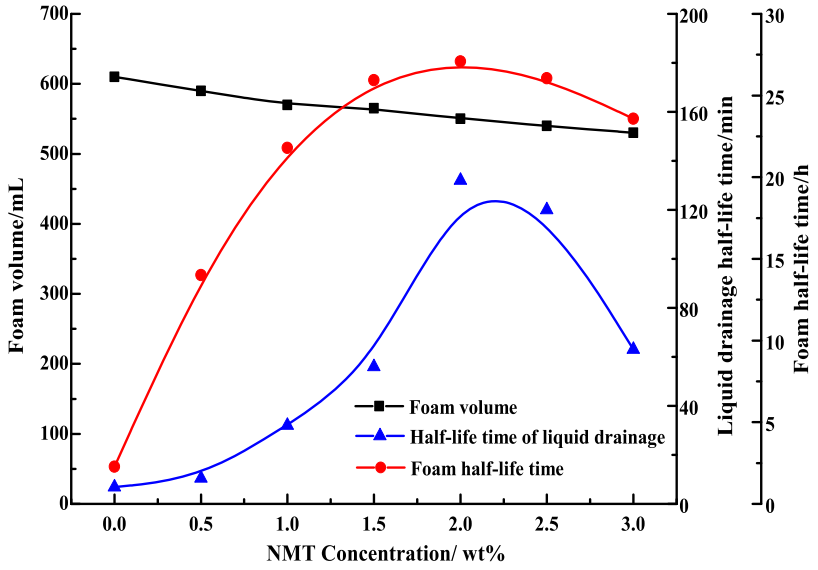

Figure 4. Foaming ability and foam stability of 0.5 wt % AOS with different concentrations of nanoclay.

foam stability of 0.5 wt % AOS with different concentrations of nanoclay NMT. As shown in Figure 4, the foam volume decreases slightly in varying degrees with the addition of nanoclay. However, it can be seen that the addition of nanoclay can significantly improve the half-life time of liquid drainage and the foam half-life time of AOS foam. When the concentration of NMT was 2.0 wt %, the liquid drainage half-life time can be extended from 408 s to 132 min and the foam half-life time can be extended from 137 min to 27.08 h.

It is indicated that the foam stability can significantly improve with the addition of nanoclay in a surfactant system. This is because the nanoclay particles can be adsorbed on the surface of the foam film to form a structure, which can make the foam more stable. The studies by Chaturvedi and Sharma have also been shown that the nanoparticles can be adsorbed on the surface of the foam and formed a multilayer from a single layer with increasing nanoparticle concentration, which strengthens the foam liquid film strength and resists bubble deformation.[31,32] The microscopy photographs of surfactant-stabilized foam and nanoclay-surfactant-stabilized foam are shown in Figure 5. It can

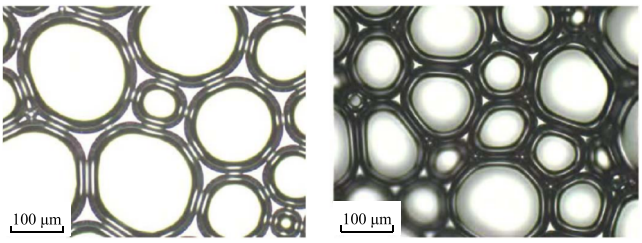

(a) Surfactant stabilized foam (b) Nanoclay-surfactant stabilized foam

Figure 5. Microscope photographs of the surfactant and nanoclay-surfactant-stabilized foam. (a) Surfactant-stabilized foam and (b) nanoclay-surfactant-stabilized foam.

be seen that the liquid film of the surfactant-stabilized foam is composed of the arrangement of surfactants, so it has a certain dynamic fluidity and cannot prevent the coalescence and Oswald ripening. From the microstructure of nanoclay-surfactant foam shown in Figure 5b, the foam formed by the nanoclay and surfactant has obvious shadows, which indicates that the nanoclay is adsorbed on the gas−liquid interface to form a solid particle film. The solid particle film structure can hinder the flow of water during liquid drainage and the Oswald ripening process to slow down the bursting of the bubble, thus improving the stability of the foam.[33−35] With the increase in concentration, more NMT particles were adsorbed on the surface of the liquid film.[36] As a result, the structural strength of the liquid film increased, which made it more difficult for the film to be thin and burst and the foam became more stable. When the concentration continued to increase, NMT would affect the Marangoni effect of foam and reduce the stability, which is reflected in the shortening of the liquid drainage half-life time and the foam half-life time.

3.1.3. Thermal Stability Evaluation. Since the temperature in steam flooding can be reached to 300 °C, the foaming and stabilizing properties of the nanoclay-surfactant-stabilized foam agent after aging at 100−300 °C were investigated. Figure 6 shows the foaming ability and foam stability of 0.5 wt % AOS + 1.0 wt % NMT after aging treatment at 100−300 °C for 24 h, which can reflect the thermal resistance of the foam system. It can be seen in Figure 6 that the foaming volume and half-life time of the liquid drainage decrease foam volume slowly with increasing temperature. However, the foam half-life time has decreased more significantly with increasing temperature, which indicated that the stability of the foam system decreased after heat aging treatment. This is mainly due to the decrease in the surface viscosity of the liquid film and the increase in the liquid film drainage rate with the increase in temperature. At the same time, the high temperature intensifies the molecular movement in the bubble and the liquid vapor pressure increases, causing the liquid film to rapidly evaporate to make it thin.

The foaming volume and half-life of the foam after heat aging treatment at 300 °C are still as high as 520 mL and 15 h, respectively, which indicated that nanoclay-surfactant-stabilized foam has good thermal resistance. This is mainly because nanoclay has good thermal resistance, and nanoclay particles were adsorbed on the surface of the liquid film to form the space barrier network structure, which can resist the coalescence and Oswald ripening of bubbles. In addition, the synergistic effect between the surfactant and nanoclay can make the molecules densely arranged to enhance the strength and elasticity of the

https://doi.org/10.1021/acsomega.1c03008
ACS Omega 2021, 6, 22709−22716

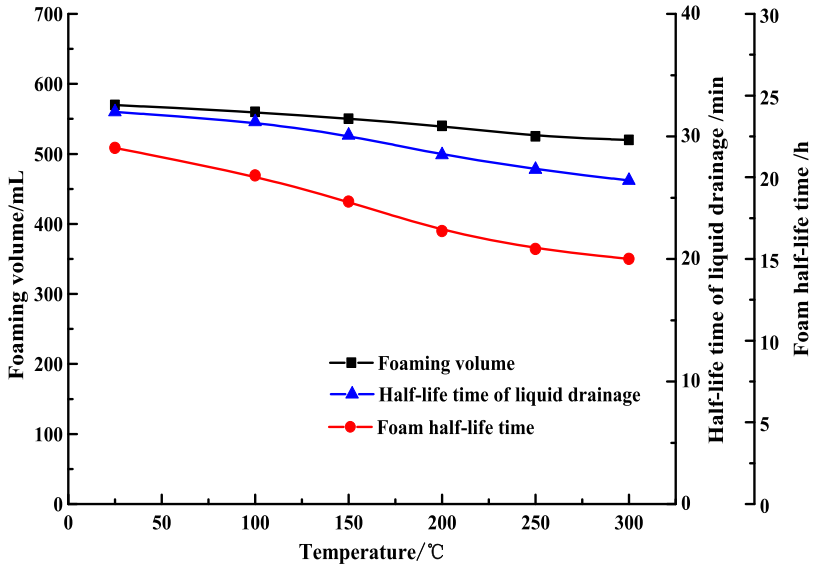

Figure 6. Foaming ability and foam stability of 0.5% AOS + 1.0% NMT at different temperatures.

liquid film, inhibiting the discrete effect caused by the intense Brownian motion of the molecules at high temperatures.

3.2. Foam Resistance Factor. Foam is a selective plugging agent, which has the characteristics of high flow resistance and high apparent viscosity in porous media. It can effectively inhibit the flow of gas and water phases and has a good profile control effect in heterogeneous reservoirs. The resistance factor is usually used to reflect the blocking ability of the foam. The resistance factor of the nanoclay-surfactant-stabilized foam in 2200 mD sandpack with different gas−liquid ratios were measured at 300 °C, as shown in Figure 7. It can be seen from

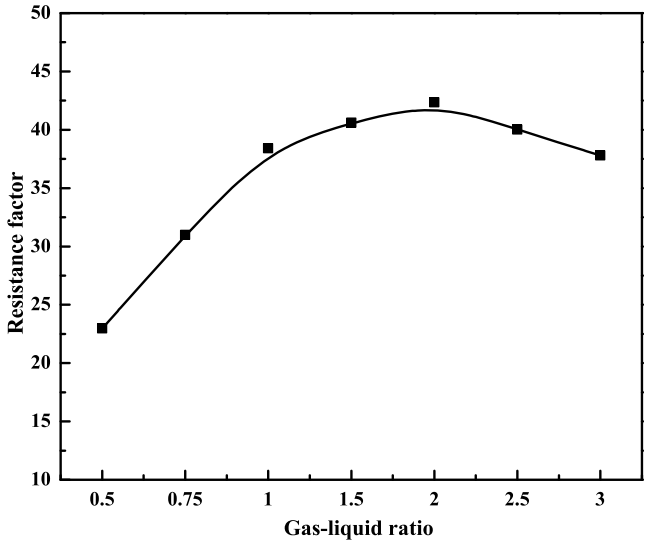

Figure 7. Resistance factor of nanoclay-surfactant-stabilized foam with different gas−liquid ratios.

Figure 7 that the resistance factor increases with increasing gas−liquid ratio. When the gas−liquid ratio is less than 1, the resistance factor increases rapidly with the increase in the gas−liquid ratio. The increasing trend of the resistance factor slows down and basically stabilizes when the gas−liquid ratio is greater than 1. This is because the apparent viscosity of the foam increases with the gas−liquid ratio, thus enhancing the blocking ability. However, the resistance factor decreases when the gas−liquid ratio is greater than 2. This is because the gas−liquid ratio is too large to easily form gas channeling, which is not conducive to foam plugging. Overall, the resistance factor of the nanoclay-surfactant-stabilized foam with different gas−liquid ratios was greater than 22 at 300 °C, which indicated that the nanoclay-surfactant-stabilized foam had good abilities of profile modification and blocking ability. The experimental results showed that the nanoclay-surfactant-stabilized foam has an optimal gas−liquid ratio of 2, and the foam resistance factor can be above 40. It is indicated that nanoclay-surfactant-stabilized foam can block the large pore of the high permeability area and divert the steam to the low permeability area. Therefore, the foam can adjust the steam injection profile and improve the sweep efficient in steam flooding.

3.3. Sandpack Flooding Tests. In order to evaluate the effectiveness of nanoclay-surfactant-stabilized foam for improving steam flooding oil recovery. A single sandpack flooding with a permeability of 2125 mD and the parallel double sandpack flooding tests with a permeability of 878 and 2533 mD were carried out. The foam system was prepared by mixing 0.5 wt % of surfactant AOS in 1.0% nanoclay NMT solution. The gas−liquid ratio was fixed at 1, and the injected foam volume was fixed at 0.5 PV. The details of the experimental parameters and the results of the sandpack flooding tests are summarized in Table 2.

Figure 8 shows the cumulative oil recovery, pressure drop, and water cut for the single sandpack flooding. During the injection of nanoclay-surfactant-stabilized foam slug, the pressure drop increase to a peak of 0.493 MPa and the water cut decreases to 51.2%. This is indicated that the nanoclay-surfactant-stabilized foam can increase the flow resistance and reflected as the peak in pressure drop during the injection of foam slug. As a result, the cumulative oil recovery increased from 59.90 to 76.42% after 0.5 PV foam was injected. The results of single sandpack flooding test show that the nanoclay-surfactant-stabilized foam can improve heavy oil recovery of steam flooding.

A parallel double sandpack flooding test with a permeability of 878 and 2533 mD was carried out to evaluate the effectiveness of nanoclay-surfactant-stabilized foam for improving oil recovery in heterogeneous heavy oil reservoirs. The foam system was 0.5 wt % AOS + 1.0 wt % NMT. The gas−liquid ratio was fixed at 1,

https://doi.org/10.1021/acsomega.1c03008
ACS Omega 2021, 6, 22709−22716

Table 2. Summary of Sandpack Flooding Tests

Type		porosity (%)	permeability (mD)	initial oil saturation (%)	steam flooding recovery (%OOIP)	tertiary recovery (% OOIP)	cumulative recovery (% OOIP)
	single sandpack	36.25	2125	92.13	59.90	16.52	76.42
double sandpacks	low permeability	30.12	878	91.89	20.36	40.54	60.90
	high permeability	38.43	2533	92.23	50.86	14.11	64.97
	total				35.97	27.01	62.98

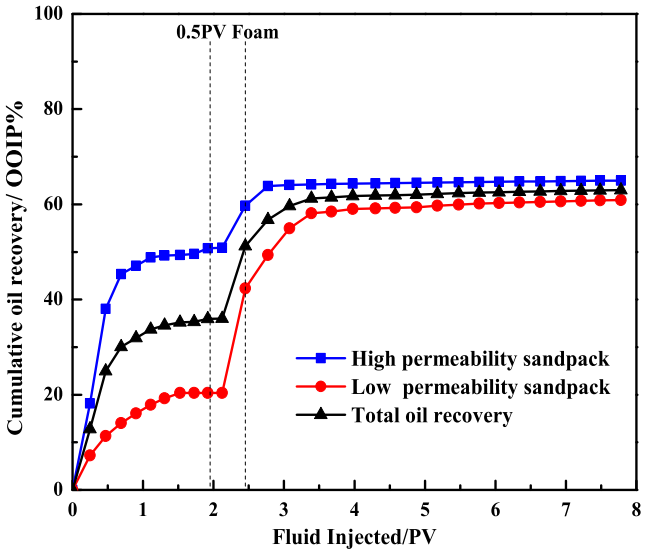

Figure 8. Result of foam assisted steam flooding in the single sandpack flooding test.

and the injected foam volume was fixed at 0.5 PV. The cumulative oil recovery of double sandpack flooding as a function of injected fluid is plotted in Figure 9.

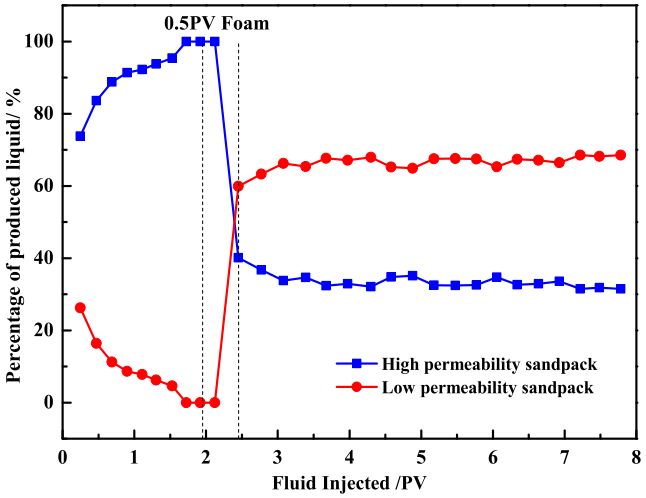

Figure 9. Cumulative recovery curve of foam assisted steam flooding in double sandpack flooding.

It can be seen from Figure 9 that the cumulative oil recovery of initial steam flooding in high-permeability sandpack can reach 50.86%, the oil recovery of steam flooding in low-permeability sandpack was only 20.36%, and the total oil recovery was only 35.97%. It indicates the steam breakthrough along high-permeability sandpack. It can be also seen from Figure 10 that the high-permeability sandpack accounts for 70% of the

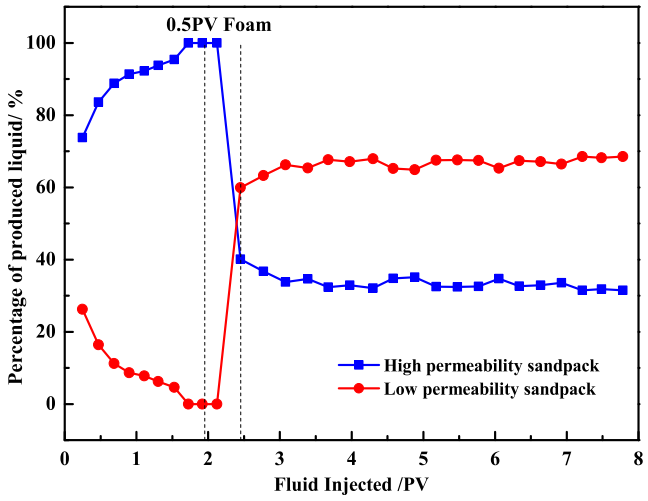

Figure 10. Percentage of produced liquid of foam-assisted steam flooding in double sandpack flooding.

produced liquid in the initial steam flooding and the low-permeability sandpack only accounts for 30%. The produced liquid of the high-permeability sandpack gradually increased to 100%, and the low-permeability sandpack gradually decreased to 0. It is indicated that the steam channeling and fingering phenomenon occurred in the high-permeability sandpack because of the low density and viscosity of the steam, which reduces the sweep efficiency of steam flooding and thus lowers the oil recovery of steam flooding in the low-permeability sandpack. Therefore, the incremental oil recovery of steam flooding can be significantly reduced due to the poor sweep efficiencies caused by the serious steam channeling and fingering in the heterogeneous heavy oil reservoirs.

After initial steam flooding, a 0.5 PV slug of nanoclay-surfactant-stabilized foam prepared with 0.5 wt % AOS + 1.0 wt % NMT was injected. It was found in Figure 10 that the produced fluid of the high-permeability sandpack decreased rapidly, while the produced fluid of the low-permeability sandpack increased rapidly. Finally, the produced fluid of the high-permeability sandpack accounted for 35% and the produced fluid of the low-permeability sandpack accounted for 65%. It is shown in Figure 9 that the oil recovery significantly increased from 20.36 to 60.90%, and the incremental recovery of 40.54% of OOIP was improved in low-permeability sandpack. As for the high-permeability sandpack, the oil recovery increased from 50.86 to 64.97% and the incremental recovery value was 14.11%. It is indicated that the nanoclay-surfactant-stabilized foam selectively enters the high-permeability sandpack and forms an effective blockage, which inhibits the steam channeling along the high-permeability sandpack so that most of the subsequent injected steam enters the low-permeability sandpack, thereby greatly improving the steam sweep efficiency in the low-permeability sandpack.

https://doi.org/10.1021/acsomega.1c03008
ACS Omega 2021, 6, 22709−22716

For heterogeneous formations, steam flooding mainly fingers along the high-permeability area due to the low steam density and viscosity, which seriously reduces the sweep efficiency of steam flooding in low-permeability sandpack.[35] By injecting the nanoclay-surfactant-stabilized foam, the foam was preferred to plugging the high-permeability sandpack and reducing the liquid flow in the high-permeability sandpack and the subsequent steam can be diverted to the low-permeability sandpack. This is because a continuous steam channel was generated in initial steam flooding, resulting in lower oil saturation and lower pressure in high-permeability sandpack. Therefore, the nanoclay-surfactant-stabilized foam prefers to flow in high-permeability sandpack. Due to high apparent viscosity and Jamin effect of the nanoclay-surfactant-stabilized foam, the resistance to steam flow can significantly increase in the high-permeability sandpack. As a result, the subsequent injected steam can be diverted to the low-permeability sandpack. This is indicated that the nanoclay-surfactant-stabilized foam can effectively improve the sweep efficiency of steam, thereby significantly improving oil recovery of steam flooding in heterogeneous heavy oil reservoirs.

4. CONCLUSIONS

(1) The foam stability and thermal resistance studies showed that the foam stability can significantly improve with the addition of the nanoclay particle NMT in an AOS surfactant system. When the concentration of nanoclay is greater than 1.0 wt %, the half-life time of liquid drainage and the foam half-life time of AOS foam can be significantly improved.

(2) The nanoclay-surfactant foam system has good performance of thermal resistance and plugging effect, and the resistance factor under 300 °C is greater than 30 when the gas−liquid ratio ranges from 1 to 3.

(3) The heterogeneous sandpack flooding showed that the nanoclay-surfactant-stabilized foam system can effectively divert the steam into the low-permeability area and increase the swept efficiency, thus improving oil recovery of steam flooding in heavy oil reservoirs.

AUTHOR INFORMATION

Corresponding Author

Wei Zheng − *CNOOC Research Institute Co. Ltd., Beijing 100028, China; State Key Laboratory of Offshore Oil Exploitation, Beijing 100028, China*; Email: zhengwei_aswill@163.com

Authors

Xianhong Tan − *CNOOC Research Institute Co. Ltd., Beijing 100028, China; State Key Laboratory of Offshore Oil Exploitation, Beijing 100028, China*

Weidong Jiang − *China National Offshore Oil Corporation, Beijing 100028, China*

Haojun Xie − *CNOOC Research Institute Co. Ltd., Beijing 100028, China; State Key Laboratory of Offshore Oil Exploitation, Beijing 100028, China*

Haihua Pei − *College of Petroleum Engineering, China University of Petroleum(East China), Qingdao 266580, China*; orcid.org/0000-0003-0010-0792

Complete contact information is available at: https://pubs.acs.org/10.1021/acsomega.1c03008

Notes

The authors declare no competing financial interest.

ACKNOWLEDGMENTS

This research was funded by the China National Offshore Oil Corporation (project no: YXKY-ZX 06 2021).

REFERENCES

(1) Lashgari, H. R.; Lotfollahi, M.; Delshad, M.; Sepehrnoori, K.; Eric de, R. *Steam-Surfactant-Foam Modeling in Heavy Oil Reservoirs*; Presented at SPE Heavy Oil Conference-Canada: Alberta, Canada, June10−12, 2014.

(2) Li, Y.-B.; Zhang, Y.-Q.; Luo, C.; Gao, H.; Li, K.; Xiao, Z.-R.; Wang, Z.-Q.; Pu, W.-F.; Bai, B. The experimental and numerical investigation of in situ re-energization mechanism of urea-assisted steam drive in superficial heavy oil reservoir. *Fuel* **2019**, *249*, 188−197.

(3) Cuenca, A.; Lacombe, E.; Chabert, M. *Impact of Oil on Steam Foam Formulations at 250°C*; Presented at SPE EOR Conference at Oil and Gas West Asia: Muscat, Oman, 21−23 March, 2016.

(4) Suhag, A.; Ranjith, R.; Balaji, K.; Peksaglam, Z.; Malik, V.; Zhang, M.; Biopharm, F. *Optimization of Steam flooding Heavy Oil Reservoirs*; Presented at SPE Western Regional Meeting: Bakersfield, California, USA, 23−27 April, 2017.

(5) Pang, Z.; Liu, H.; Zhu, L. A laboratory study of enhancing heavy oil recovery with steam flooding by adding nitrogen foams. *J. Petrol. Sci. Eng.* **2015**, *128*, 184−193.

(6) Hosseini-Nasab, S. M.; Zitha, P. L. J. Investigation of Chemical-Foam Design as a Novel Approach toward Immiscible Foam Flooding for Enhanced Oil Recovery. *Energy Fuels* **2017**, *31*, 10525−10534.

(7) Pang, S.; Pu, W.; Wang, C. A Comprehensive Comparison on Foam Behavior in the Presence of Light Oil and Heavy Oil. *J. Surfactants Deterg.* **2018**, *21*, 657−665.

(8) Bagheri, S. R.; Clark, H. P. *Steam-Foam Technology as an Option to Improve Steam Drive Efficiency*; Presented at SPE Kuwait Oil & Gas Show and Conference: Mishref, Kuwait, 11−14 October, 2015.

(9) Wang, Y.; Wang, H.; Zhao, X.; Li, C.; Luo, J.; Sun, S.; Hu, S. Effect of hydrophobically modified SiO_2 nanoparticles on the stability of water-based SDS foam. *Arabian J. Chem.* **2020**, *13*, 6942−6948.

(10) Du, Q.; Liu, H.; Wu, G.; Hou, J.; Zhou, K.; Liu, Y. Application of flue-gas foam in thermal-chemical flooding for medium-depth heavy oil reservoirs. *Energy Sci. Eng.* **2019**, *7*, 2936−2949.

(11) Telmadarreie, A.; Trivedi, J. J. CO_2 Foam and CO_2 Polymer Enhanced Foam for Heavy Oil Recovery and CO_2 Storage. *Energies* **2020**, *13*, 5735.

(12) Zhao, G.; Dai, C.; Zhang, Y.; Chen, A.; Yan, Z.; Zhao, M. Enhanced foam stability by adding comb polymer gel for in-depth profile control in high temperature reservoirs. *Colloids Surf., A* **2015**, *482*, 115−124.

(13) Bashir, A.; Haddad, A. S.; Rafati, R. Nanoparticle/polymer-enhanced alpha olefin sulfonate solution for foam generation in the presence of oil phase at high temperature conditions. *Colloids Surf., A* **2019**, *582*, 123875.

(14) Tyowua, A. T.; Binks, B. P. Growing a particle-stabilized aqueous foam. *J. Colloid Interface Sci.* **2020**, *561*, 127−135.

(15) AlYousef, Z.; Almobarky, M.; Schechter, D. Enhancing the stability of foam by the use of nanoparticles. *Energy Fuels* **2017**, *31*, 10620−10627.

(16) AlYousef, Z. A.; Almobarky, M. A.; Schechter, D. S. The effect of nanoparticle aggregation on surfactant foam stability. *J. Colloid Interface Sci.* **2018**, *511*, 365−373.

(17) Alzobaidi, S.; Lotfollahi, M.; Kim, I.; Johnston, K. P.; DiCarlo, D. A. Carbon dioxide-in-brine foams at high temperatures and extreme salinities stabilized with silica nanoparticles. *Energy Fuels* **2017**, *31*, 10680−10690.

(18) Du, D.; Zhang, X.; Li, Y.; Zhao, D.; Wang, F.; Sun, Z. Experimental study on rheological properties of nanoparticle-stabilized carbon dioxide foam. *J. Nat. Gas Sci. Eng.* **2020**, *75*, 103140.

(19) Guo, F.; Aryana, S. An experimental investigation of nanoparticle-stabilized CO_2 foam used in enhanced oil recovery. *Fuel* **2016**, *186*, 430−442.
(20) Yekeen, N.; Idris, A. K.; Manan, M. A.; Samin, A. M. Experimental study of the influence of silica nanoparticles on the bulk stability of SDS-foam in the presence of oil. *J. Dispersion Sci. Technol.* **2016**, *38*, 416−424.
(21) Khajehpour, M.; Etminan, S. R.; Goldman, J.; Fred, W. *Nanoparticles as Foam Stabilizer for Steam-Foam Process*; Presented at SPE EOR Conference at Oil and Gas West Asia: Muscat, Oman 21−23, March, 2016.
(22) Mohd, T. A. T.; Harun, A.; Ghazali, N. A.; Alias, N.; Yahya, E. Interfacial Tension Dependence on Nanoparticle Surface Modification for Stabilization of CO_2 Foam in EOR: An Overview. *Adv. Mater. Res.* **2015**, *1113*, 637−642.
(23) Bashir, A.; Sharifi Haddad, A.; Rafati, R. *Experimental Investigation of Nanoparticles/Polymer Enhanced CO_2-Foam in the Presence of Hydrocarbon at High-Temperature Conditions*; Presented at SPE International Heavy Oil Conference and Exhibition: Kuwait City, Kuwait, 10−12, December, 2018.
(24) Li, W.; Wei, F.; Xiong, C.; Ouyang, J.; Shao, L.; Dai, M.; Liu, P.; Du, D. A Novel supercritical CO_2 foam system stabilized with a mixture of zwitterionic surfactant and silica nanoparticles for enhanced oil recovery. *Front. Chem.* **2019**, *7*, 718.
(25) Fu, C.; Liu, N. Study of the synergistic effect of the nanoparticle-surfactant-polymer system on CO_2 foam apparent viscosity and stability at high pressure and temperature. *Energy Fuels* **2020**, *34*, 13707−13716.
(26) Fu, C.; Yu, J.; Liu, N. Nanoparticle-stabilized CO_2 foam for waterflooded residual oil recovery. *Fuel* **2018**, *234*, 809−813.
(27) Rezaei, A.; Derikvand, Z.; Parsaei, R. Surfactant-silica nanoparticle stabilized N_2-foam flooding: A mechanistic study on the effect of surfactant type and temperature. *J. Mol. Liq.* **2021**, *325*, 115091.
(28) Bera, A.; Mandal, A.; Belhaj, H.; Kumar, T. Enhanced oil recovery by nonionic surfactants considering micellization, surface, and foaming properties. *Petrol. Sci.* **2017**, *14*, 362−371.
(29) Rognmo, A. U.; Heldal, S.; Fernø, M. A. Silica nanoparticles to stabilize CO_2-foam for improved CO_2 utilization: Enhanced CO_2 storage and oil recovery from mature oil reservoirs. *Fuel* **2018**, *216*, 621−626.
(30) Liu, Q.; Zhang, S.; Sun, D.; Xu, J. Foams stabilized by Laponite nanoparticles and alkylammonium bromides with different alkyl chain lengths. *Colloids Surf., A* **2010**, *355*, 151−157.
(31) Chaturvedi, K. R.; Sharma, T. In-situ formulation of pickering CO_2 foam for enhanced oil recovery and improved carbon storage in sandstone formation. *Chem. Eng. Sci.* **2021**, *235*, 116484.
(32) Chaturvedi, K. R.; Narukulla, R.; Trivedi, J.; Sharma, T. Effect of single-step silica nanoparticle on rheological characterization of surfactant based CO_2 foam for effective carbon utilization in subsurface applications. *J. Mol. Liq* **2021**, 116905.
(33) Chaturvedi, K. R.; Sharma, T. Rheological analysis and EOR potential of surfactant treated single-step silica nanofluid at high temperature and salinity. *J. Petrol. Sci. Eng.* **2021**, *196*, 107704.
(34) Fameau, A.-L.; Salonen, A. Effect of particles and aggregated structures on the foam stability and aging. *Compt. Rendus Phys.* **2014**, *15*, 748−760.
(35) Hurtado, Y.; Franco, C. A.; Riazi, M.; Cortés, F. B. Improving the stability of nitrogen foams using silica nanoparticles coated with polyethylene glycol. *J. Mol. Liq.* **2020**, *300*, 112256.
(36) Chaturvedi, K. R.; Trivedi, J.; Sharma, T. Single-step silica nanofluid for improved carbon dioxide flow and reduced formation damage in porous media for carbon utilization. *Energy* **2020**, *197*, 117276.

https://doi.org/10.1021/acsomega.1c03008
ACS Omega 2021, 6, 22709−22716